IEEE Access
Multidisciplinary | Rapid Review | Open Access Journal

IEEE POWER & ENERGY SOCIETY SECTION

Received 13 October 2023, accepted 8 November 2023, date of publication 13 November 2023,
date of current version 28 November 2023.

Digital Object Identifier 10.1109/ACCESS.2023.3332469

RESEARCH ARTICLE

A Robust Distributed State Estimation of AC/DC System With LCC-HVDC Tie Line

HAIBO ZHANG, (Senior Member, IEEE), HOUYU QI, AND SHUAI WANG, (Member, IEEE)
State Key Laboratory of Alternate Electrical Power System with Renewable Energy Sources, North China Electric Power University, Beijing 102206, China
Corresponding author: Houyu Qi (qhyopen@163.com)

ABSTRACT A robust distributed state estimation algorithm for AC/DC system with AC tie lines and high voltage direct current (LCC-HVDC) tie lines is proposed. The proposed algorithm consists of robust DC state estimation in the coordinator and robust distributed AC state estimation, and implements sequential solving by exchanging coupling variables of the AC/DC system. For AC state estimation, a distributed state estimation algorithm based on the bilinear algorithm is designed, which can achieve the same accuracy as the centralized algorithm. Robust state estimator based on the exponential absolute value function and exponential square function is suitable for reducing the influence of outliers and can reduce the operation scale by simplifying the nonlinear iterative process in distributed state estimation. Finally, the correctness and effectiveness of the algorithm is verified by simulation of three IEEE 118 bus systems interconnected through AC/DC hybrid tie lines.

INDEX TERMS Distributed state estimation, bilinear state estimation, robust state estimation, AC/DC systems, LCC-HVDC.

I. INTRODUCTION

State estimation (SE) is a prerequisite for many applications in the energy management system (EMS), providing input data for economic dispatch, optimal power flow, contingency analysis *etc* [1]. So, it is an essential part of modern EMS, which ensures the stable and secure operation of the power system [2], [3], [4]. The goal of power system state estimation is to provide state estimates of bus voltages information based on the raw measurements collected by the supervisory control and data acquisition (SCADA) system or phasor measurement units (PMUs) [5]. The requirements of data privacy in each control center and the heavy calculation load make it more and more difficult for integrated state estimation (ISE) to adapt to large-scale network. Distributed computing may be a more sensible choice [6]. Distributed state estimation (DSE) allows each aggregate bus or control area to have its own processor for local state estimation, control area only need to exchange a small amount of data with each other and can obtain results with the same accuracy as integrated computing [7].

The distributed state estimation algorithm can be divided into hierarchical state estimation and decentralized state estimation. Almost all distributed algorithms are refined on the two architectures to assure global convergence and enhance computing efficiency.

Fully decentralized state estimation [8], [9], [10], [11], [12], [13], [14], [15] does not need a coordinator, and each subsystem only exchange data with adjacent subsystems. However, fully decentralized algorithm requires data exchanges with high communication costs and has slow rate of convergence because it has more information being exchanged and needs more iterations compared to the hierarchical algorithm [14].

Hierarchical state estimation is usually a two-level structure [16], [17]. In the first level, each subsystem estimates the states according to its local measurements and uploads the boundary information to the coordinator. In the second level, the coordinator combines the estimated boundary states and boundary measurements to estimate the boundary states

The associate editor coordinating the review of this manuscript and approving it for publication was Elizete Maria Lourenco.

© 2023 The Authors. This work is licensed under a Creative Commons Attribution-NonCommercial-NoDerivatives 4.0 License.
For more information, see https://creativecommons.org/licenses/by-nc-nd/4.0/

again. The traditional two-level state estimation only pays attention to the coordination of boundary states and does not involve the correction of the calculation results from subsystems, making it unable to obtain the global optimal solution. Lagrange multiplier method can be used to improve the traditional structure [18]. The coordinator modified the internal calculation results from each subsystem after the calculation of the boundary variables of each region. On this basis, the algorithm with weight updating [19] was proposed to effectively improve the estimation quality. The sensitivity of the local objective function to the boundary state [20] was used to replace the boundary variables for lessening the amount of data exchange. To reduce the frequency of data exchange between two levels, the distributed parallel sub-regions and tie-line state estimation were adopted [21]. The sub-region calculations were corrected according to the sensitivity matrix coordination algorithm and the regional tie-line state estimation result. The hierarchical state estimation algorithm can more efficiently use the information of each region and effectively realize multi-region parallel state estimation for faster convergence and lower communication cost.

There are several complications arising from distributed state estimation. First, the received measurements may contain bad data. Robust state estimation can identify these bad measurements and weaken its impact on estimation results. Maximum exponential absolute value state estimation [22] and exponential objective function state estimation [22], [23] are common robust algorithms. They can curtail the weight of bad data through nonlinear iteration and automatically suppress the influence of bad data and model deviation. In order to improve the efficiency of the cost function, a new robust state estimator based on the exponential absolute value function and the quadratic cost function is proposed for power system state estimation which obtains smaller state estimation errors under non-Gaussian measurement noise [24].

Another problem faced by the distributed state estimation algorithm is the influence of the DC system. All of the algorithms mentioned above are only used in AC systems. With the development of HVDC technology, many HVDC project have been widely implemented, forming a large-scale AC/DC interconnected power grid. The research on distributed state estimation algorithms for AC/DC power grids mainly focuses on AC/DC microgrids interconnected by DC tie lines [11], [25], [26], [27], [28], instead of the system with AC/DC hybrid tie lines. Besides, the above methods neglect the coordinated correction of boundary bus power and voltage amplitude and the acquisition of DC sub-region reference values [28].

In this paper, a robust distributed state estimation algorithm for AC/DC systems with AC tie lines and HVDC tie lines is proposed to wrestle with the two complications. The major contributions of this study are as follows:

(1) A new distributed algorithm architecture for AC/DC systems with AC tie lines and HVDC tie lines is proposed. The robust DC state estimation (DC SE) is set in the coordinator, exchanges coupling variables with AC system to achieve alternating solutions, so the information exchange between AC and DC systems takes place at coordinator. Only AC system needs distributed computing. The distributed AC state estimation (AC SE) does not involve convergence problem, and only exchanges data twice. The total number of information exchange only depends on the number of alternating solutions between AC and DC systems.

(2) The bilinear robust algorithm [15] is adopted to resist the influence of bad measurements. The influence of outliers can be reduced by the weight matrix by linear iteration based on the proposed robust state estimator. Nonetheless, the bilinear algorithm leads to the appearance of repeated measurements. Therefore, the corresponding solution to the problem of repeated measurement is also proposed, which can be replaced by its relationship with other measurements.

(3) In the bilinear state estimation, the reference bus acquisition of the AC system is implemented in the second linear state estimation, but it is not suitable for AC/DC hybrid systems. Thus, a reference bus selection method is proposed to obtain unified reference values of each AC/DC subsystem.

The overall structure of the paper is as follows: Section II introduces the overall computing architecture of the algorithm, and the model for both the AC state estimation and DC state estimation. Section III introduces the principle of the distributed computing mechanism. Section IV supplements the details of distributed computing. Section V discusses the method for bad data suppression. Section VI provide the whole process for the robust distributed AC/DC state estimation algorithm. Section VII provides some test results to verify the effect of the algorithm.

II. THE CALCULATION ARCHITECTURE OF THE ALGORITHM

The solution for AC/DC state estimation can be divided into the unified method [29] and the sequential method [30]. In the unified method, the state variables of AC system and DC system are included in a unified objective function and solved iteratively at the same time. The sequential method divides AC/DC state estimation into AC SE and DC SE, which is then solved sequentially. In the sequential solution, AC SE and DC SE need to exchange boundary variables. When the exchanged variables are within a certain error range, the AC/DC state estimation converges. Besides, the convergence speed of this alternating solution is faster.

According to the sequential method, AC SE and DC SE are solved independently and sequentially. The DC SE of all DC tie lines is carried out in the coordinator. For AC SE, the DC tie line is regarded as load S_{DC} at the point of common coupling (PCC) bus, so each subsystem only calculates the AC SE of the local AC power grid. Each subsystem needs to exchange the equivalent information to coordinator after local AC SE calculation. When the distributed AC SE is completed, each subsystem sends PCC voltage to the coordinator, and

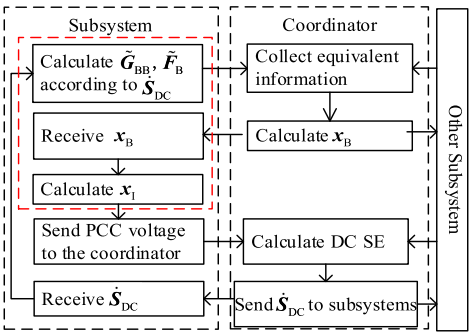

FIGURE 1. Computing architecture of the algorithm.

the coordinator calculates the DC SE according to the PCC voltage. The above calculation process is repeated until the change of PCC voltage and power is small enough. The distributed computing structure is shown in Fig. 1.

In Fig.1, PCC voltage refers to the voltage at the connection point of AC/DC system; The power injection into DC system S_{DC} refers to the power flowing from AC system to DC system. $\tilde{G}_{BB}$ and $\tilde{F}_B$ are the equivalent information matrix and vector. x_B is the global boundary states vector which contains the boundary states of the whole system. As shown in Fig. 1, distributed AC/DC state estimation can be divided into distributed AC SE of subsystem (The dotted red box in Fig. 1) and DC SE calculation in the coordinator. The calculation model of AC SE and DC SE are introduced in the following section.

A. STATE ESTIMATION OF DC SYSTEM

The schematic diagram of a typical two-terminal LCC-HVDC transmission system is as follows:

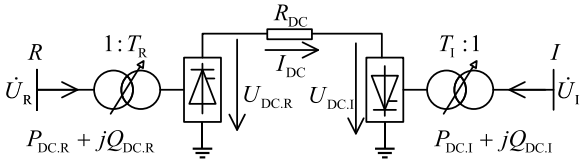

FIGURE 2. Model of a two-terminal LCC-HVDC.

As shown in Fig. 2, a DC system is composed of the converter, converter transformer and DC transmission line (its resistance is R_{DC}). The connection points between AC system and DC system are defined as PCC buses (namely R and I in Fig. 1). The direction of power flowing from AC system to DC system through PCC buses is set as the positive direction, therefore, the power flow at the PCC bus is defined as the power injection into DC system. The PCC voltage and power injection into DC system are the exchange variables between AC SE and DC SE in the sequential method.

In steady-state conditions, rectifier equations can be expressed as follows:

$$U_{DC0.R} = \frac{3\sqrt{2}}{\pi} T_R U_R \tag{1-1}$$

$$U_{DC.R} = U_{DC0.R} cos\alpha - \frac{3}{\pi} X_{C.R} I_{DC} \tag{1-2}$$

$$cos\phi_R = U_{DC.R}/U_{DC0.R} \tag{1-3}$$

$$P_{DC.R} = U_{DC.R} I_{DC} \tag{1-4}$$

$$Q_{DC.R} = U_{DC.R} I_{DC} tan\phi_R \tag{1-5}$$

where $U_{DC.R}$ is the PCC voltage at the rectifier side, $U_{DC0.R}$ is the no-load DC voltage, T_R is the converter transformer's ratio on the rectifier side, $X_{C.R}$ is the commutated reactance and ϕ_R is the power factor angle on the rectifier side. The subscripts "R" in the above variables represent that they are variables on the rectifier side, and replacing "R" in these subscripts with "I" indicate that they are inverter side variable. I_{DC} is the current. α is the ignition delay angle of the rectifier side.

The inverter, just like the rectifier has similar equations, distinguished by the subscript "I":

$$U_{DC0.I} = \frac{3\sqrt{2}}{\pi} T_I U_I \tag{2-1}$$

$$U_{DC.I} = U_{DC0.I} cos\gamma - \frac{3}{\pi} X_{C.I} I_{DC} \tag{2-2}$$

$$cos\phi_I = U_{DC.I}/U_{DC0.I} \tag{2-3}$$

$$P_{DC.I} = -U_{DC.I} I_{DC} \tag{2-4}$$

$$Q_{DC.I} = U_{DC.I} I_{DC} tan\phi_I \tag{2-5}$$

where γ represents the extinction advance angle on the inverter side. Also, the relationship between DC voltage and current is as follows:

$$U_{DC.R} - U_{DC.I} = I_{DC} R_{DC} \tag{3}$$

For DC system, if the converter transformer's ratio and DC voltage are known, the rest variables of DC system can be solved. Therefore, these variables can be defined as state variables of DC SE. Furthermore, in order to simplify the form of measurement equations, some other variables are also defined as state variables. To sum up, the state variables set of DC system is as follows:

$$x_{DC} = \left[U_{DC.R}\ U_{DC.I}\ \ T_R\ T_I\ \ \phi_R\ \phi_I\ \ I_{DC}\ \alpha\ \gamma\ \right]^T \tag{4}$$

Measurements from DC system includes the power injection into DC system, converter transformer's ratio, DC voltage and current, as shown in equation (5-1)-(5-9).

$$U_{DC.R}^{mea} = U_{DC.R} + \varepsilon \tag{5-1}$$

$$U_{DC.I}^{mea} = U_{DC.I} + \varepsilon \tag{5-2}$$

$$I_{DC}^{mea} = I_{DC} + \varepsilon \tag{5-3}$$

$$P_{DC.R}^{mea} = U_{DC.R} I_{DC} + \varepsilon \tag{5-4}$$

$$P_{DC.I}^{mea} = -U_{DC.I} I_{DC} + \varepsilon \tag{5-5}$$

$$Q_{DC.R}^{mea} = U_{DC.R} I_{DC} tan\phi_R + \varepsilon \tag{5-6}$$

$$Q_{DC.I}^{mea} = U_{DC.I} I_{DC} tan\phi_I + \varepsilon \tag{5-7}$$

$$T_R^{mea} = T_R + \varepsilon \tag{5-8}$$

$$T_I^{mea} = T_I + \varepsilon \tag{5-9}$$

where ε represents the measurement deviation. According to equation (1-1)-(3), the DC system also has the following

virtual measurements:

$$0 = I_{DC} - \frac{U_{DC.R} - U_{DC.I}}{R_{DC}} + \varepsilon \tag{6-1}$$

$$0 = cos\phi_R - \frac{U_{DC.R}}{\frac{3\sqrt{2}}{\pi} T_R U_R} + \varepsilon \tag{6-2}$$

$$0 = cos\phi_I - \frac{U_{DC.I}}{\frac{3\sqrt{2}}{\pi} T_I U_I} + \varepsilon \tag{6-3}$$

$$0 = U_{DC.R} + \frac{3}{\pi} X_{C.R} I_{DC} - \frac{3\sqrt{2}}{\pi} T_R U_R cos\alpha + \varepsilon \tag{6-4}$$

$$0 = U_{DC.I} + \frac{3}{\pi} X_{C.I} I_{DC} - \frac{3\sqrt{2}}{\pi} T_I U_I cos\gamma + \varepsilon \tag{6-5}$$

The virtual measurement equation (6-1)-(6-5) contains the state variables of AC system, i.e., the PCC voltage U_R, which needs to be updated by AC SE. In addition, the control equations of DC system will also be used as measurements in the DC SE. Taking the control mode of constant current at rectifier side and constant extinction angle at inverter side as an example, the corresponding measurement equation is as follows:

$$I_{DC}^{C.mea} = I_{DC} + \varepsilon \tag{6-1}$$

$$\gamma^{C.mea} = \gamma + \varepsilon \tag{6-2}$$

The measurement equations corresponding to other control modes can be derived from the equations of DC system and will not be repeated. It should be noted that the control equation gives an accurate value of state variables, so these measurements should be given a higher weight in the DC SE calculation.

B. OVERVIEW OF THE BILINEAR STATE ESTIMATION ALGORITHM

The bilinear state estimation (BSE) [15] is adopted to estimate the state of AC system. By introducing auxiliary state variables and auxiliary measurements, bilinear state estimation achieves accurate linearization of measurement equation. BSE consists of two linear state estimation (LSE-1 and LSE-2) stages and a nonlinear transformation stage. In the conventional state estimation algorithm, the voltage amplitude and phase angle of the bus are selected as the state variables, and the measurement equations of the state variables are nonlinear.

While in the first stage (LSE-1), the new state variables of LSE-1 are defined as follows:

$$J_i = U_i^2 \tag{8-1}$$

$$K_{ij} = U_i U_i cos\theta_{ij} \tag{8-2}$$

$$L_{ij} = U_i U_i sin\theta_{ij} \tag{8-3}$$

U_i and θ_{ij} are the magnitude and phase angle difference of the bus voltage. Based on the above definition of state variables, the measurement equation of conventional measurement for new state variables is a linear equation.

$$P_i^{mea} = \sum_{j \in i} \left(G_{ij} K_{ij} + B_{ij} L_{ij}\right) + G_{ii} J_i + P_{DC.i} \tag{9-1}$$

$$Q_i^{mea} = \sum_{j \in i} \left(G_{ij} L_{ij} - B_{ij} K_{ij}\right) - B_{ii} J_i + Q_{DC.i} \tag{9-2}$$

where G_{ij} and B_{ij} are the conductance and susceptance of row i and column j of the node admittance matrix, $P_{DC.i}$ and $Q_{DC.i}$ are the active and reactive power injection into the DC system. According to the alternating solution method, they are regarded as constant when solving AC SE.

In the second stage (nonlinear transformation), the measurements of LSE-2 can be obtained by nonlinear transformation of the estimation results of LSE-1:

$$\alpha_i^{mea} = lnJ_i \tag{10-1}$$

$$\alpha_{ij}^{mea} = \ln\left(K_{ij}^2 + L_{ij}^2\right) \tag{10-2}$$

$$\theta_{ij}^{mea} = acrtan\left(L_{ij}^2 / K_{ij}^2\right) \tag{10-3}$$

The variable with "$\wedge$" represents the optimal estimates of state variables.

In the third stage (LSE-2), lnU_i and θ_i are defined as the state variables of LSE-2, and the measurement equation of LSE-2 is expressed as follows:

$$\alpha_i^{mea} = 2lnU_i + \varepsilon \tag{11-1}$$

$$\alpha_{ij}^{mea} = 2lnU_i + 2lnU_i + \varepsilon \tag{11-2}$$

$$\theta_{ij}^{mea} = U_i - U_j + \varepsilon \tag{11-3}$$

The objective function of LSE-1 and LSE-2 both have the following form:

$$min_{\boldsymbol{x}} J(\boldsymbol{x}) = (\boldsymbol{Z} - \boldsymbol{A}\boldsymbol{x})\, \boldsymbol{W}\, (\boldsymbol{Z} - \boldsymbol{A}\boldsymbol{x}) \tag{12}$$

where $\boldsymbol{A}$ is the measurement coefficient matrix, $\boldsymbol{W}$ is the weight matrix, $\boldsymbol{Z}$ is the measurement vector, and $\boldsymbol{x}$ is the state variables vector. The optimal estimates of state variables in LSE-1 and LSE-2 satisfy the linear equations:

$$\boldsymbol{A}^T W A x = \boldsymbol{A}^T W Z \tag{13}$$

The above equation is a linear equation, so the optimal estimate can be solved by the following equations:

$$\hat{\boldsymbol{x}} = \left(\boldsymbol{A}^T \boldsymbol{W} \boldsymbol{A}\right)^{-1} \boldsymbol{A}^T W Z \tag{14}$$

There are two advantages of using the bilinear algorithm. One of the important features is that the measurement equations of the voltage amplitude and phase angle are decoupled in LSE-2, so their state estimates can be performed separately. Based on this characteristic, the LSE-2 is also highly computationally efficient. Another advantage is that there is no need to choose initial values for the iteration, as they are simply and reliably provided by LSE-1. Therefore, as long as the result of LSE-1 is accurate, the LSE-2 virtually yields the optimal solution after a single run of the three-stage procedure. This is also the reason why robust state estimation is performed only in LSE-1 in section V. This result was verified in reference [12], and we also carry out simulation tests to verify this in Section VII.

In summary, bilinear state estimation only needs to solve two linear problems to get the optimal state estimates. At the

same time, the algorithm does not involve the convergence problem, so it does not need to perform iterative calculation.

III. THE PRINCIPLE OF THE ALGORITHM

A. AC SE OF THE SUBSYSTEM

According to the distributed computing structure mentioned in Section II, the DC SE of all DC tie lines is carried out in the coordinator. Therefore, each subsystem only needs to model the internal AC network and regards the DC system as a load. Take the interconnection system with two subsystems as an example, in which the modeling of subsystem 1 is as shown in Fig. 3 below.

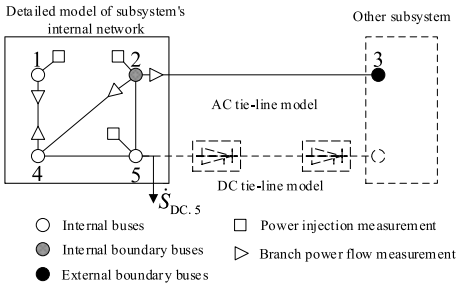

FIGURE 3. Model of subsystem 1.

Because the DC tie-line is modeled in the coordinator and is regarded as a load in the subsystem's AC SE, DC tie line model is represented by the dotted line in Fig. 3. Each subsystem will model the internal network and the AC tie-line in detail. Because the AC tie-line is modeled repeatedly in different subsystems, its terminals are defined as boundary buses. Further, the boundary buses near the internal network are defined as the internal boundary buses, while the boundary buses on the external network side are defined as external boundary buses. The measurements from the subsystem are divided in a non-overlapping way: the power flow measurement near the internal boundary buses is divided into the subsystem, and the measurement near the external boundary buses is divided into the adjacent subsystem. The measurements of DC system and branch power flow measurement at the PCC bus are incorporated into the coordinator.

The measurements of different subsystems will involve the same state variables, namely boundary state variables. The boundary state variables' definition of LSE-1 and LSE-2 is different. In LSE-1, the tie-line power flow measurement is related to the state variables of the subsystems on both sides, so it is defined as boundary states. Taking subsystem 1 of Fig. 3 as an example, the boundary states of LSE-1 are as follows:

$$x_{B_1}^{LSE-1} = \begin{bmatrix} K_{23} & L_{23} \end{bmatrix}^T \tag{15}$$

In LSE-2, the state variables of the internal and external boundary buses of the subsystem are defined as the boundary states.

$$x_{B_1}^{LSE-2} = \begin{bmatrix} lnU_2 & lnU_3 & \theta_2 & \theta_3 \end{bmatrix}^T \tag{16}$$

B. DISTRIBUTED COMPUTING MECHANISM BASED ON EQUIVALENT INFORMATION DATA EXCHANGE

Since bilinear state estimation includes two linear state estimation, the distributed AC SE can be discussed with linear estimation model. The linear equation (13) satisfied by the optimal solution of linear state estimation can be shortened as follows:

$$Gx = F \tag{17}$$

$\boldsymbol{G}$ is defined as information matrix and $\boldsymbol{F}$ is defined as the information vector. Taking three subsystems as an example, the global state vector is arranged in order such that the internal state variables of each subsystem comes first and the global boundary state variables comes second:

$$x = \begin{bmatrix} x_{I_1}^T & x_{I_2}^T & x_{I_3}^T & x_B^T \end{bmatrix}^T \tag{18}$$

where x_{I_i} is the internal state variables of subsystem i, x_B is the global boundary state variables, that is, the union of the boundary state variables of all subsystems.

We partition the row of $\boldsymbol{A}$ and $\boldsymbol{Z}$ according to the measurement of subsystem, and partition the column of $\boldsymbol{A}$ according to the state variables arrangement of (18). It should be noted that the premise of this block form is that different subsystems do not contain the same measurements.

$$\boldsymbol{Z} = \begin{bmatrix} \boldsymbol{Z}_1 \\ \boldsymbol{Z}_2 \\ \boldsymbol{Z}_3 \end{bmatrix}, \boldsymbol{A} = \begin{bmatrix} \boldsymbol{A}_{1.I_1} & & & \boldsymbol{A}_{1.B} \\ & \boldsymbol{A}_{2.I_2} & & \boldsymbol{A}_{2.B} \\ & & \boldsymbol{A}_{3.I_3} & \boldsymbol{A}_{3.B} \end{bmatrix}$$
$$W = \begin{bmatrix} W_1 & & \\ & W_2 & \\ & & W_3 \end{bmatrix} \tag{19}$$

In the above equation, $A_{i.I_j}$ is the measurement coefficient matrix of subsystem i to the internal state of subsystem j. Since the measurement of subsystem i has nothing to do with the internal state variables of other subsystems, when i is not equal to j, matrix $A_{i.I_j}$ is a zero matrix. $A_{i.B}$ is the measurement coefficient matrix of subsystem i with respect to the global boundary states, W_i is the equivalent weight matrix, its specific calculation formula is in (38).

Combining (18)-(19), we can get the block matrix form of (17) as shown in (20):

$$\begin{bmatrix} G_{I_1I_1} & & & G_{I_1B} \\ & G_{I_2I_2} & & G_{I_2B} \\ & & G_{I_3I_3} & G_{I_3B} \\ G_{BI_1} & G_{BI_2} & G_{BI_3} & GBB \end{bmatrix} \begin{bmatrix} x_{I_1} \\ x_{I_2} \\ x_{I_3} \\ x_B \end{bmatrix} = \begin{bmatrix} F_{I_1} \\ F_{I_2} \\ F_{I_3} \\ F_B \end{bmatrix} \tag{20}$$

The calculation formulas of block matrices and vectors are as follows:

$$G_{I_iI_i} = A_{i,I_i}^T W_i A_{i,I_i} \tag{21-1}$$
$$G_{I_iB} = A_{i,I_i}^T W_i A_{i,B} \tag{21-2}$$
$$G_{BB} = \sum_{i=1}^{3} A_{i,B}^T W_i A_{B,i} = \sum_{i=1}^{3} G_{(i)BB} \tag{21-3}$$
$$F_{I_i} = A_{i,I_i}^T W_i Z_i \tag{21-4}$$

$$F_B = \sum_{i=1}^{3} A_{i,B}^T W_i Z_i = \sum_{i=1}^{3} F_{(i)B} \tag{21-5}$$

$G_{(i)BB}$ and $F_{(i)B}$ are the blocks of the information matrix and the information vector at the position of the boundary states, and are calculated by subsystem i.

By retain the global boundary state variables in (20) and eliminate the internal state variables of the subsystems according to gauss elimination method, the following equivalent equations can be obtained.

$$\tilde{G}_{BB} x_B = \tilde{F}_B \tag{22}$$

In (22), $\tilde{G}_{BB}$ and $\tilde{F}_B$ are the global equivalent boundary information matrix and global equivalent boundary information vector respectively. In terms of solving x_B, (22) and (20) are completely equivalent. After obtaining x_B, the subsystem can calculate the internal state variables by using the following formula according to its own measurements:

$$G_{I_l I_i} x_{I_l} = F_{l_l} - G_{I_l B} x_B \tag{23}$$

Combined with (20) and the principle of equivalent calculation, the calculation formulas of $\tilde{G}_{BB}$ and $\tilde{F}_B$ are as follows:

$$\tilde{G}_{BB} = \sum_{i=1}^{3} \left(G_{(i)BB} - G_{BI_i} G_{I_i I_i}{}^{-1} G_{I_i B} \right) \tag{24-1}$$

$$\tilde{F}_B = \sum_{i=1}^{3} \left(F_{(i)B} - G_{BI_i} G_{I_i I_i}{}^{-1} F_{I_i} \right) \tag{24-2}$$

Since the summation terms in the above equations are only related to the information of each subsystem, (24-1) and (24-2) can also be written in the following form:

$$\tilde{G}_{BB} = \sum_{i=1}^{3} \tilde{G}_{(i)BB} \tag{25-1}$$

$$\tilde{F}_B = \sum_{i=1}^{3} \tilde{F}_{(i)B} \tag{25-2}$$

$\tilde{G}_{(i)BB}$ and $\tilde{F}_{(i)B}$ are the internal equivalent information matrix and the internal equivalent information vector respectively of subsystem i. According to the above discussion, the internal equivalent information $\tilde{G}_{(i)BB}$ and $\tilde{F}_{(i)B}$ can be calculated independently by each subsystem, and then (25-1) and (25-2) can be obtained at the coordinator and then x_B can be calculated. The dimension of $\tilde{G}_{(i)BB}$ and $\tilde{F}_{(i)B}$ is not high, and the data amount is acceptable in the distributed calculation environment. When each subsystem obtains the estimated value of the state variables by distributed calculation, the PCC voltage magnitude (belonging to the internal state variables of the subsystem) is uploaded to the coordinator, and the coordinator calculates the DC SE according to the PCC voltage magnitude uploaded by each subsystem. Then the injected power of PCC bus is obtained by DC SE and transferred to adjacent subsystems for AC SE. The distributed AC SE of subsystems and DC SE of coordinator are carried out sequentially until the exchanged data variation is small enough.

IV. DETAILED IMPLEMENT OF THE ALGORITHM

A. REPEATED MEASUREMENTS IN DIFFERENT SUBSYSTEM

Equation (19) partitions the matrix on the premise that the measurements of each subsystem are not repeated. LSE-1 satisfies this condition because the measurements are divided by non-overlapping partition method. However, LSE-2 does not satisfy this condition because the boundary state variables (tie-line's state variables K_{ij} and L_{ij}) of each subsystem in LSE-1 will be transformed to the repeated boundary measurements (α_{ij} and θ_{ij}) in LSE-2 by nonlinear transformation. Therefore, if $\boldsymbol{Z}$ is still partitioned according to subsystem, the measurement vector Z^o corresponding to repeat measurements must be subtracted from global measurement $\boldsymbol{Z}$, otherwise the repeat measurement will be counted twice in the objective function. Accordingly, the measurement coefficient matrix A^o corresponding to repeated measurement also should be subtracted from the measurement coefficient matrix $\boldsymbol{A}$.

$$Z = \begin{bmatrix} Z_1 \\ Z_2 \\ Z_3 \end{bmatrix} - Z^o, A = \begin{bmatrix} A_{1.I_1} & & & A_{1.B} \\ & A_{2.I_2} & & A_{2.B} \\ & & A_{3.I_3} & A_{3.B} \end{bmatrix} - A^o \tag{26}$$

Z_o is the repeated measurement vector of the whole system, that is, the branch power flow measurement of all tie-lines (α_{ij} and θ_{ij}). These measurements are only related to the global state variables x_B. A^o is the repeat measurement coefficient matrix of the whole system.

The objective function of LSE-2 can be expressed in the following form:

$$\begin{aligned} \min J(x) = &\sum_{i=1}^{3} [Z_i - A_i x]^T W_i [Z_i - A_i x] \\ &- [Z^o - A^o x] W^o [Z^o - A^o x] \end{aligned} \tag{27}$$

Z_i and A_i respectively represent the measurement vector and measurement coefficient matrix of subsystem i, where Z_i of different subsystems contains the same measurement. Note that A_i is a matrix of measurement coefficients for the state variables of the whole network.

Because the repeated measurements are only related to the boundary state variables of the whole network. In the information matrix and information vector corresponding to repeated measurement, only the partition matrix G_{BB}^o and the partition vector F_{BB}^o are not zero. So, (22) needs to be modified to (28):

$$(\sum_{i=1}^{3} \tilde{G}_{(i)BB} - G_{BB}^o) x_B = \sum_{i=1}^{3} \tilde{F}_{(i)B} - F_B^o \tag{28}$$

The equivalent information of LSE-2 can be calculated as follows:

$$\tilde{G}_{BB} = \sum_{i=1}^{3} \left(G_{(i)BB} - G_{BI_i} G_{I_i I_i}^{-1} G_{I_i B} \right) - G_{BB}^{\circ} \tag{29-1}$$

$$\tilde{F}_B = \sum_{i=1}^{3}\left(F_{(i)B} - G_{BI_i}G_{I_iI_i}^{-1}F_{I_i}\right) - F_{BB}^{\circ} \tag{29-2}$$

Let $G_{(i)BB}^{o}$ and $F_{(i)B}^{o}$ represent the partition of the information matrix and information vector corresponding to the repeated boundary measurements of subsystem i at the boundary state varies. Since repeated boundary measurements are only possible in two subsystems, the following equation can be obtained:

$$2G_{BB}^{o} = \sum_{i=1}^{3} G_{(i)BB}^{o} \tag{30-1}$$

$$2F_{B}^{o} = \sum_{i=1}^{3} F_{(i)B}^{o} \tag{30-2}$$

Therefore, the formula of the whole network equivalent information matrix and the whole network equivalent information vector can be transformed into a form similar to LSE-1:

$$\tilde{G}_{BB} = \sum_{i=1}^{3} G_{(i)BB} - \frac{1}{2}G_{(i)BB}^{\circ} = \sum_{i=1}^{3} G_{(i)BB} \tag{31-1}$$

$$\tilde{F}_{B} = \sum_{i=1}^{3} F_{(i)B} - \frac{1}{2}F_{i,B}^{0} = \sum_{i=1}^{3} \tilde{F}_{(i)B} \tag{31-2}$$

In the above formula, the summation term $\tilde{G}_{(i)BB}$ and $\tilde{F}_{(i)B}$ are only related to the internal information of subsystems and can be calculated independently.

B. SELECTION OF THE REFERENCE BUS

In the distributed state estimation algorithm, the selection of reference bus is an important problem to be discussed. In this paper, the reference bus is determined by the coordinator. In LSE-2, each subsystem calculates the internal equivalent information without a reference bus. After receiving the internal equivalent information of all subsystems, the coordinator obtains the equivalent elements shown in (31-1)-(31-2), and selects a boundary bus as the reference bus to solve the boundary state variables. When the subsystem calculates the internal state variables according to (23), its reference bus is determined as the boundary bus selected by the coordinator, therefore, all subsystem have the same reference bus.

C. COMPUTATIONAL EFFICIENCY ANALYSIS OF THE DSE FRAMEWORK

Computational efficiency is related to the number of data exchanges and the amount of data exchanges.

For the analysis of the number of exchanges, the distributed computing of the AC system does not involve the convergence problem, and only requires two data exchanges, so the total number of information exchanges only depends on the number of alternating solutions between the AC and DC systems. Generally, the convergence speed of the alternating solution is fast, so the total information exchange times of the algorithm is less.

The amount of data exchanged by each subsystem is another concern of distributed computing. Explain the meaning of the subscript in $\tilde{G}_{(i)BB}$, $\tilde{F}_{(i)B}$, $\tilde{G}_{(i)B_iB_i}$ and $\tilde{F}_{(i)B_i}$ firstly. "(i)" means that this is the equivalent information of subsystem i, "B_i" represents the boundary variables corresponding to subsystem i, and "B" represents the boundary variables of the whole network. It should be noted that the subsystem's boundary state variables x_{B_i} is only a subset of the whole network boundary state variables x_B, so $\tilde{G}_{(i)BB}$ and $\tilde{F}_{(i)B}$ are nonzero only the parts corresponding to their boundary state variables x_{B_i}, as shown in the Fig. 4.

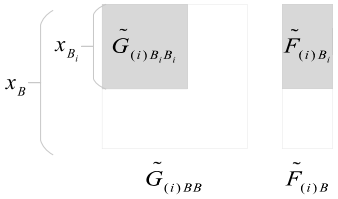

FIGURE 4. Subsystem actual equivalent information matrix and equivalent information vector.

In actual calculation, each subsystem only needs to transmit $\tilde{G}_{(i)B_iB_i}$ and $\tilde{F}_{(i)B_i}$ when transmitting $\tilde{G}_{(i)BB}$ and $\tilde{F}_{(i)B}$.The dimensions of the equivalent information matrices $\tilde{G}_{(i)B_iB_i}$ and the equivalent information vectors $\tilde{F}_{(i)B_i}$ are the number of boundary state variables. And $\tilde{G}_{(i)B_iB_i}$ is a symmetric matrix that only needs to transmit the upper or lower trigonometric elements. In LSE-1, the boundary state variables of the subsystem are the state variables of the connect line. The total number is twice the number of the contact line, and the amount of data is not large. In addition, in the distributed state estimation of AC-DC system, the injected power of DC system only affects the equivalent information vector $\tilde{F}_{(i)B_i}$, so the equivalent information matrix $\tilde{G}_{(i)B_iB_i}$ only needs to be uploaded once, and the subsequent coordinator can be reused.

The situation with LSE-2 is slightly different. If the measurement of LSE-2 is regarded as a branch, the measurement coefficient matrix is basically equivalent to the transposition of the node-branch incidence matrix, so the information matrix in LSE-2 has a structure similar to that of the subsystem node admittance matrix:

$$(A_i^{sub})^T W_i A_i^{sub} = \begin{bmatrix} G_{I_iI_i} & G_{I_iBI_i} & \\ G_{BI_iI_i} & G_{BI_iBI_i} & G_{BI_iBE_i} \\ & G_{BE_iBI_i} & G_{BE_iBE_i} \end{bmatrix} \tag{32}$$

In (32), A_i^{sub} is the measurement coefficient matrix of subsystem i for its own state variables, which should be distinguished from A_i mentioned above; The subscript I_i, BI_i and BE_i of the block information matrix represent the internal bus state variables, the internal boundary bus state variables and the external boundary bus state variables of subsystem i respectively. By equivalent transformation of (32), the internal and external boundary bus state variables

are retained and the internal bus state variables are eliminated, so the equivalent information matrix can be obtained:

$$\tilde{G}_{B_iB_i} = \begin{bmatrix} \tilde{G}_{BI_iBI_i} & G_{BI_iBE_i} \\ G_{BE_iBI_i} & G_{BE_iBE_i} \end{bmatrix} \tag{33}$$

According to (33), only G_{BI_i,BI_i} needs to be modified in the equivalent information matrix, while other matrix blocks are the same as before the equivalence. G_{BI_i,BI_i} is also a symmetric matrix that only need to upload the upper or lower trigonometric elements. In the subsystem, there is no branch connection between the external boundary bus, so G_{BE_i,BE_i} is a diagonal matrix, and all the elements are 0 except the diagonal elements. G_{BI_i,BE_i} is also a sparse matrix, and the elements at ij are not 0 only if there is a connection relationship between bus i and j. Similar to LSE-1, the equivalent information matrix only needs to be uploaded once, and only the equivalent information vector needs to be updated later.

In general, the amount of data transmitted by subsystem and coordinator is within the acceptable range, and the equivalent information does not involve the detailed data inside the subsystem, which is suitable for application in distributed computing environment.

V. BAD DATA SUPPRESSION

The robust state estimation algorithm can automatically suppress measurement errors in the process of state estimation. The maximum exponential square (MES) robust state estimation algorithm [23] is widely adopted in AC system to suppress bad data. Different from traditional bad data identification, the MES method can suppress bad data without any extra bad data identification loop and it also has good calculation efficiency. However, the window width of MSE has a small optional range. The maximum exponential absolute value state estimation (MEAV) [22] uses Laplace window instead of Gauss window. Compared with the maximum exponential square model, the window width has a wider selection range. But it has non-derivable points that make it hard to solve.

Fig. 5 shows the derivatives of cost functions $\partial J/\partial \varepsilon_i$ of weighted least squares (WLS), MES and MEAV with respect to measurement deviations ε_i/σ_i. According to the Fig. 5, MES has better sensitivity than WLS when measurement residuals are small. Besides, MEAV is less sensitive to the outliers especially when the measurement residual is larger, which is conducive to reducing the influence of outliers on state estimation.

In this paper, a robust estimator based on the exponential absolute value function and the exponential square function is proposed. The proposed robust estimator can be implemented by minimizing the following function:

$$J(x) = -\sum_{i=1}^{m} \rho_E\left(\varepsilon_i\right) \tag{34-1}$$

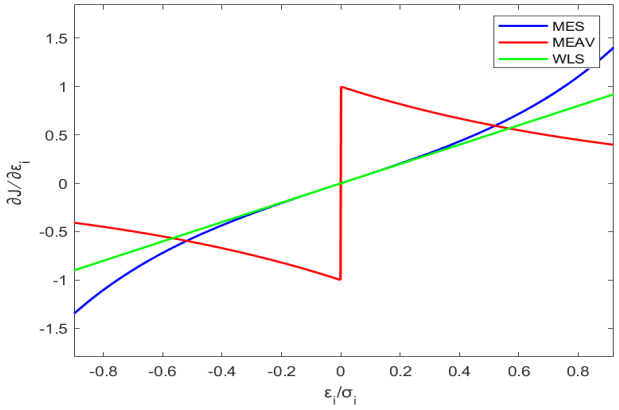

FIGURE 5. The derivatives of cost functions of different estimators.

where ρ_E is given by

$$\rho_E\left(\varepsilon_i\right) = \begin{cases} -\exp\left(-a_i - \dfrac{\varepsilon_i^2}{2\sigma_i^2}\right), & |\varepsilon_i| < a_i\sigma_i \\ -\exp\left(-\left|\dfrac{\varepsilon_i}{\sigma_i}\right| - \dfrac{a_i^2}{2}\right), & |\varepsilon_i| > a_i\sigma_i \end{cases} \tag{34-2}$$

The parameter σ is the window width. When the width is narrow, the estimated value of state variables is close to the true value, but it is hard to achieve the global optimal solution because of the local optimal points. When the width is wide, the local optimal points disappeared, but the global optimal results may deviate from the true value. To get the best robust estimation effect, the window width needs to be adjusted gradually from wide to narrow. In this paper, we adjust the window as shown in the following equation:

$$\sigma^{(k+1)} = 0.9 * \sigma^k \tag{35}$$

The optimal estimation should satisfy the following conditions:

$$\sum_{i=1}^{m} \frac{\partial \rho_E\left(\varepsilon_i\right)}{\partial \varepsilon_i} \frac{1}{\varepsilon_i} \varepsilon_i \frac{\partial \varepsilon_i\left(x\right)}{\partial x} = 0 \tag{36}$$

The equation above can be transformed to the following matrix form:

$$\left[A^T \tilde{W}(x) A\right] x = A^T \tilde{W}(x) Z \tag{37}$$

In (37), $\tilde{W}(x)$ is defined as an equivalent weight matrix, which is a diagonal matrix, and its diagonal elements are a function of state variables which are shown in (38).

$$\tilde{w}_i(x) = \begin{cases} \dfrac{\exp\left(-a_i - \frac{\varepsilon_i^2}{2\sigma_i^2}\right)}{\sigma_i^2}, & |\varepsilon_i| < a_i\sigma_i \\ \dfrac{\exp\left(-\left|\frac{\varepsilon_i}{\sigma_i}\right| - \frac{a_i^2}{2}\right)}{\sigma_i\varepsilon_i}, & |\varepsilon_i| > a_i\sigma_i \end{cases} \tag{38}$$

Equation (37) can be solved iteratively, as shown in equation (39).

$$x^{(k+1)} = \left[A^T \tilde{W}\left(x^k\right) A\right]^{-1} A^T \tilde{W}\left(x^k\right) Z \tag{39}$$

The superscript k in equation (39) represents the number of iterations. $W(x^{(k)})$ is the weight matrix, whose diagonal elements are the function of the state variables, as shown in (38).

Because all DC tie lines' DC SE is calculated in the coordinator, the robust DC SE does not need to do distributed calculation. The bad data from DC system can also be processed based on the above robust estimation, and the equivalent weight principle can also be used for iterative solution.

The coordination between robust estimation and alternating AC/DC state estimation is also a problem that needs to be paid attention to. In the state estimation of AC system, the DC system is regarded as a constant load S_{DC} (the initial value is set to 0). For the robust estimation of AC system, S_{DC} generally does not have much impact. The PCC voltage U_{PCC} is obtained after the robust estimation of AC system. Similarly, U_{PCC} has little influence on the robust estimation of DC system in general. Therefore, the robust estimation of AC system and DC system respectively only needs to be carried out once. After the measurement weight matrix is determined according to the first robust estimation, the weight matrix will be used in the subsequent calculation. In this way, it is not necessary to carry out robust estimation in every alternating AC/DC calculation.

VI. THE WHOLE PROCESS OF THE ROBUST DISTRIBUTED AC/DC STATE ESTIMATION ALGORITHM

To sum up, the whole algorithm flow is as follows:

1) Initialize the AC system parameters: $\sigma^{(0)} = 10$, $\tilde{W}(x^{(0)}) = E$, convergence criteria $\sigma^{set} = 0.01$. Initialize the DC system parameters: $\sigma^{(0)} = 10$, $\lambda^{(0)} = \pi^{(0)} = 0$ and $u^{(0)}, v^{(0)}, \alpha^{(0)}, \beta^{(0)} > 0$ and convergence criteria $\sigma^{set} = 0.01$. Set $U_{PCC(0)} = 1, S_{DC(0)} = 0$, convergence criteria $\varepsilon = 0.01$.
2) The injected power of DC state estimation S_{DC} is received from the coordinator, ready for AC state estimation.
3) Update window width $\sigma^{(k)}$, residual ε_i and weight matrix $\tilde{W}(x^{(k)})$.
4) Perform LSE-1 according to the updated weight.
5) The convergence flags of internal state variables in each subsystem are judged and uploaded, received the convergence flags of other subsystems at the same time. If one of the flags does not converge, go back to step 3), else proceed to steps 6).
6) If $\sigma^{(k)} > \sigma^{set}$, go back to step 3), else proceed to steps 7).
7) The measurements of LSE-2 are obtained by nonlinear transformation according to the optimal estimates of LSE-1.
8) LSE-2 is performed according to the measurements obtained from the nonlinear transformation.
9) Each subsystem sends PCC voltage U_{PCC} to the coordinator and the coordinator prepares for DC SE.
10) The PCC voltage is received from each subsystem and starts to perform the DC robust state estimation. Determine the equivalent weight matrix and get the DC system injected power.
11) Conventional distributed state estimation of AC/DC system is carried out according to fixed weight matrix. The only need is to continue with steps (2) - (10) and skip step (3) and (6). All the weights in the formula are replaced by the weights obtained in the first robust calculation.

Fig. 6 shows the flow chart of the algorithm. It should be noted that only the first robust calculation needs to be iterated. After the weight matrix is fixed, the conventional distributed state estimation only needs to skip the steps in the red dotted frame. The specific steps of LSE-1 and LSE-2 are also shown in Fig. 6 with dotted blue frame.

VII. SIMULATION RESULTS

A. THE TEST CASE WITHOUT BAD DATA

We interconnected three IEEE 118 bus systems with tie lines to construct the test system. The schematic diagram of the test system is shown in Fig. 7.

The control mode of DC connection line 103(R)-330(I) is that the rectifier side setting current is 0.63p.u. and the inverter side setting arc extinction angle is 17°. The control mode of DC connection line 26(R)-150(I) is 0.42p.u. of rectifier side setting current and 1.28p.u. of inverter side setting DC voltage. The measurements are obtained by adding a Gaussian noise with a standard deviation of 0.001 to the power flow calculation results. We formed 20 groups of samples according to the Monte Carlo analysis method. The control mode of these DC tie lines is constant control current on the rectifier side and constant control extinction advance angle on the inverter side. The distributed algorithm and integrated algorithm are used to estimate the state of the system. Fig. 8 shows the error of the centralized and distributed state estimation results from the 20 samples, maximum and average absolute measurements error ($|\Delta U_k|$, $|\Delta U_{avr}|$), are used as index to evaluate the performance of the state estimation method. Fig. 9 shows the comparison of computing time between the distributed state estimation algorithm proposed in this paper and the traditional centralized state estimation algorithm. Table 1 shows the error of the DC system estimation result in one set of samples.

It can be seen from the measurement sets that the results of the distributed computing are almost the same as that of the integrated calculation. At the same time, the calculation time is greatly reduced.

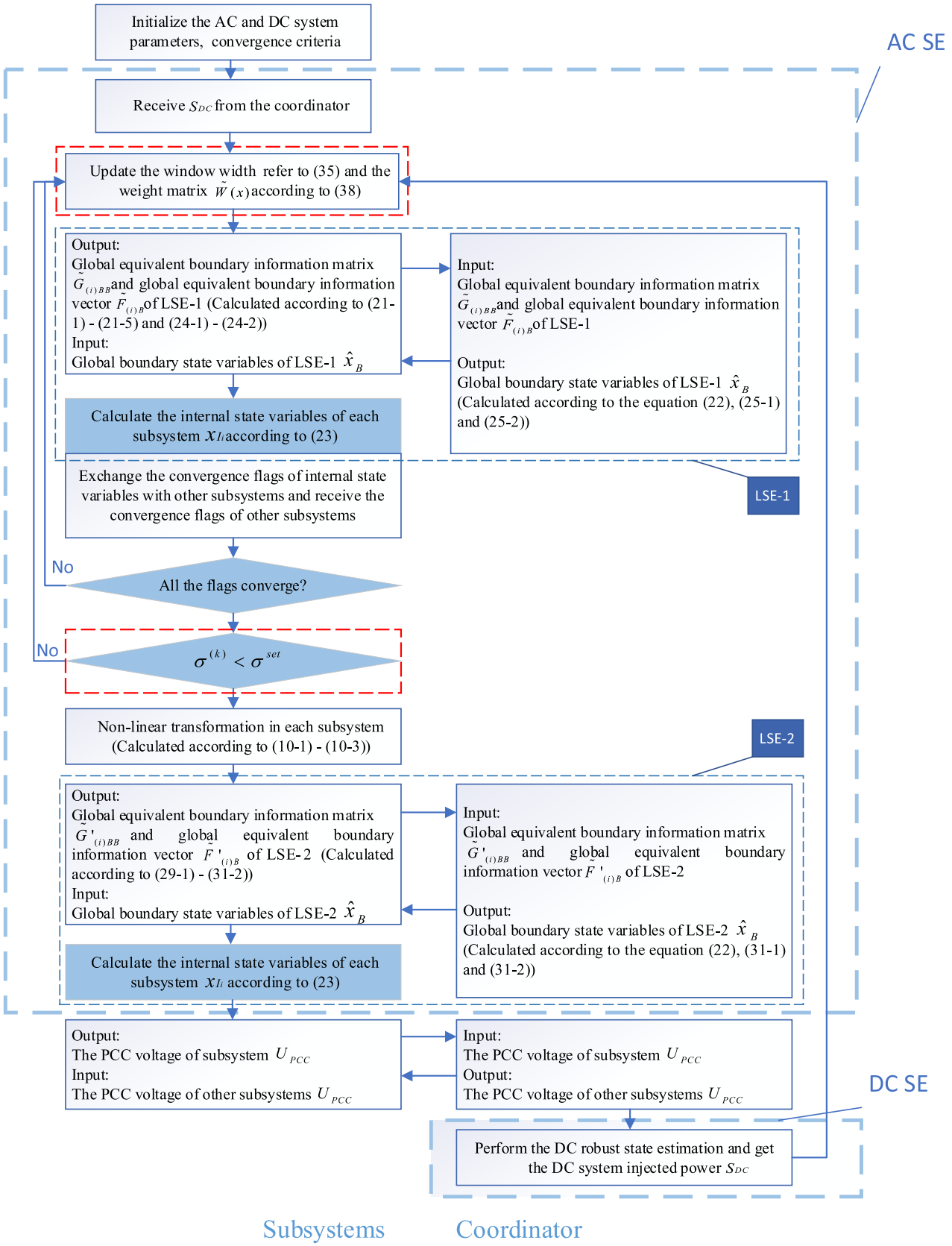

FIGURE 6. The flow chart of the algorithm.

TABLE 1. The difference of state variables between DSE and ISE.

State variables of DC system	DC tie line103(R)-330(I)		DC tie line26(R)-150(I)	
DC voltage (p.u.)	-4.3079×10^{-7}	-4.3104×10^{-7}	5.6100×10^{-9}	5.8200×10^{-9}
Converter transformer's ratio	-1.6151×10^{-8}	9.1540×10^{-8}	-1.1797×10^{-8}	-6.9520×10^{-9}
Power factor (°)	-1.5311×10^{-5}	2.5701×10^{-7}	1.2545×10^{-5}	8.0329×10^{-5}
DC current (p.u.)	6.3230×10^{-9}		4.1370×10^{-9}	
Control angle (°)	-9.84×10^{-6}	-9.80×10^{-9}	1.4707×10^{-5}	9.9853×10^{-5}

TABLE 2. Robust state estimation results of DC system.

Error measurements	True value	Estimated measurement value of DSE	Estimated measurement value of RDSE
Active power injection into DC system at bus 330	-0.780469	-0.381036	-0.779464
Reactive power injection into DC system at bus 150	0.183521	0.383427	0.186146

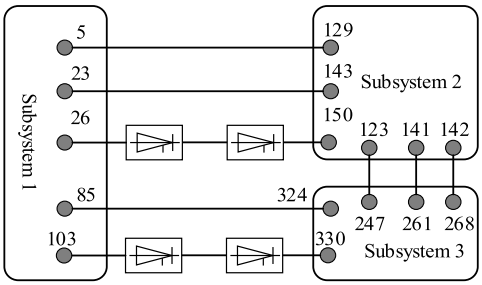

FIGURE 7. Schematic diagram of the test system.

B. THE TEST CASE CONTAINING BAD DATA

The bad measurements are constructed to test the effect of bad data suppression. The error measurements are constructed by adding a Gaussian noise whose standard deviation is 100 times of the normal measurement on the true value. 3% rate of bad measurements is added in the AC system. In DC system, one measurement is randomly selected as a bad data measurement in each DC tie line. We randomly generated 20 measurement samples containing the above error data. In the AC system's state estimation, the following two statistical parameters C1 and C2 are defined to measure the quality of the state estimation.

$$C_1 = \frac{1}{n}\sum_{i=1}^{n}\left|\hat{U}_i - U_i^*\right| \tag{40-1}$$

$$C_2 = \frac{N_{3\sigma}}{N}\times 100\% \tag{40-2}$$

$N_{3\sigma}$ is the number of measurements whose difference between the estimated value and the true value is in the range of $\pm 3\sigma$, and N is the total number of measurements. The smaller the index C_1 is, the better the estimation effect is. The larger the value of indicator C_2 the better estimation effect. Fig.8 below shows the comparison between distributed state estimation (DSE) and distributed robust estimation (RDSE).

The bad data in DC system is set in DC line 26(R) -150(I) and DC line 103(R)-330(I). Table 2 lists the comparison between conventional and robust estimation method of DC SE in a specific sample.

It can be seen from Fig. 10, in all 20 samples, the C1 of robust SE is smaller and the C2 of robust SE is larger compared with the conventional estimation method. Above all, combined with Table 2, the robust estimation can suppress the influence of bad data and can improve the quality of state estimation. We added the following error measurements to subsystem 1 to test the bad suppression effect for the boundary region.

1)Active power injection at bus 26 in the internal boundary of subsystem 1.

2) Active power injection at the internal boundary bus 85 of subsystem 1.

3) Power flow of tie-line 23-143.

4) Active power injection into DC system at PCC bus 26.

The estimated results of error measurements are shown as Table 3. According to Table 3, the estimated value of error measurement is close to the true value, and it is not affected by the error measurements, which reflects the suppression ability of the algorithm for the boundary error measurement.

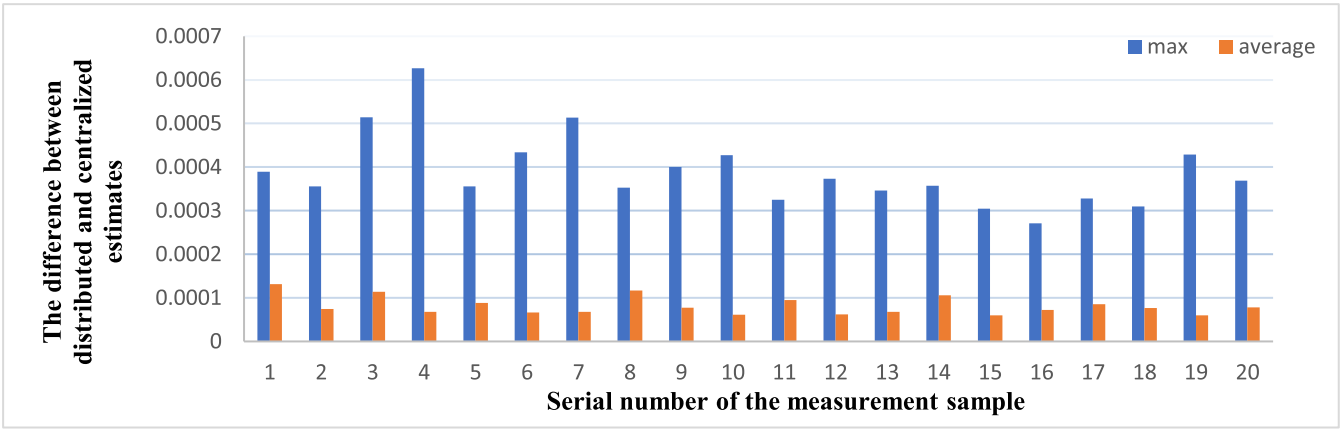

FIGURE 8. The $|\Delta U_k|$ and $|\Delta U_{avr}|$ of the 20 samples.

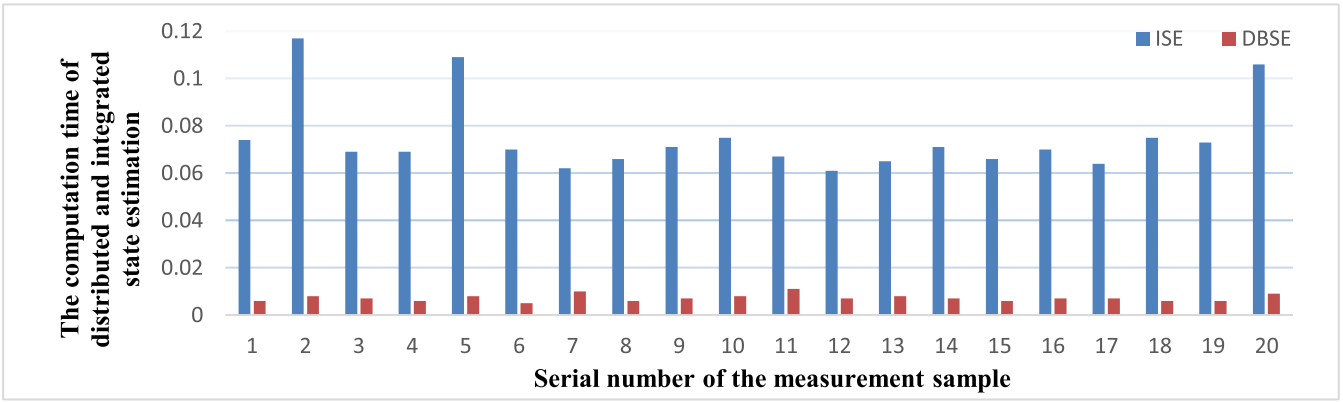

FIGURE 9. Computation time comparison of the distributed and centralized state estimates for 20 samples.

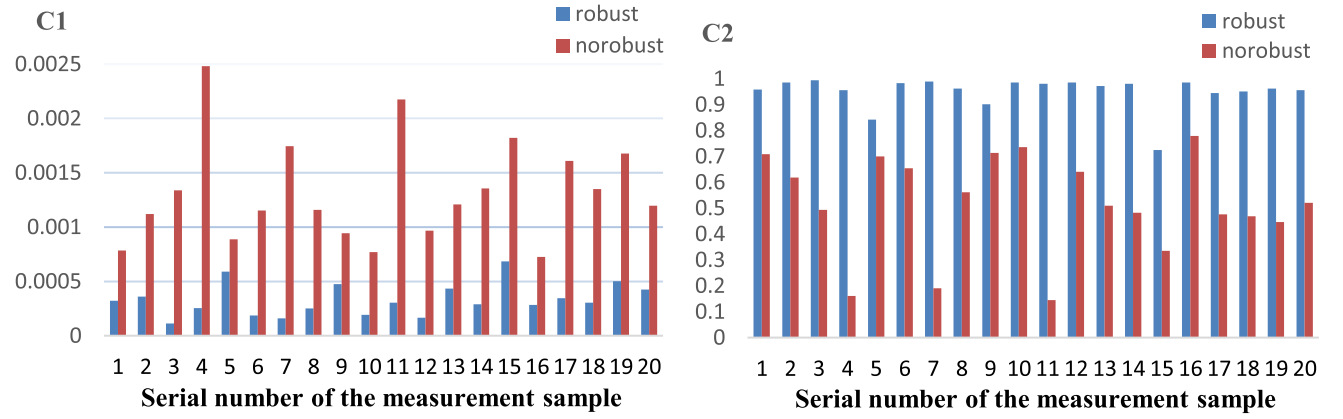

FIGURE 10. The C1 and C2 of DSE and RDSE of the 20 examples.

In order to verify that it is not necessary to add the robust algorithm to LSE-2, we select sample 4 at random and add the robust algorithm to its LSE-2. Table 4 lists the calculation time of each stage in detail. In actual operation, the sensitivity matrix is fixed after the first AC/DC iteration, so only the time spent in the first AC/DC iteration needs to be considered. Table 4 shows that the LSE-2 adds a long extra computing time, but the obtained C1, C2 statistical parameters is basically the same. Therefore, it is not necessary to add a robust algorithm to LSE-2.

TABLE 3. Estimated results of error measurements.

Error measurements	True value	Error value	Estimated value
Active power injection at bus 26	3.1400	-3.1416	3.1395
Active power injection at bus 85	-0.2400	-0.4420	-0.2406
Branch power flow of tie-line 23-143	-1.0323	-2.0325	-1.0326
Active Power injection into DC system at bus 26	0.5468	0.8472	0.5476

TABLE 4. Calculation time of each stage.

	The first alternating solution				The second alternating solution				C1	C2
	LSE-1	nonlinear transformation	LSE-2	DC SE	LSE-1	nonlinear transformation	LSE-2	DC SE		
Computation time of LSE-2 with robust algorithm(s)	0.104	0.001	0.863	0.004	0.002	0.001	0.004	0.005	0.000214	95.8271 %
Computation time of LSE-2 without robust algorithm(s)	0.104	0.001	0.003	0.004	0.002	0.001	0.004	0.005	0.000255	95.6403 %

VIII. CONCLUSION

In view of the shortcomings of traditional centralized state estimation, a distributed robust estimation algorithm of AC/DC system is proposed. The proposed algorithm can be applied to hybrid AC/DC tie-line system. The decomposition of AC SE and DC SE is realized by alternating solution. Distributed AC SE adopts the bilinear algorithm, subsystems and coordinator only need to exchange a small amount of data twice to achieve the solution, which has high reliability. In addition, this paper also solves the problem of repeated measurements and reference bus selection caused by the bilinear algorithm. Moreover, the designed piecewise robust state estimator which has the advantage of MSE and MEAV is used in the proposed distributed AC/DC state estimation method to process the bad measurement data at the boundary in distributed calculation way and realize the suppression of bad data.

REFERENCES

[1] A. J. Wood and B. F. Wollenberg, *Power Generation, Operation, and Control*. Hoboken, NJ, USA: Wiley, 1984.

[2] I. Mohammed, S. J. Geetha, S. S. Shinde, K. Rajawat, and S. Chakrabarti, "Modified re-iterated Kalman filter for handling delayed and lost measurements in power system state estimation," *IEEE Sensors J.*, vol. 20, no. 7, pp. 3946–3955, Apr. 2020.

[3] H. Yang, R. C. Qiu, L. Chu, T. Mi, X. Shi, and C. M. Liu, "Improving power system state estimation based on matrix-level cleaning," *IEEE Trans. Power Syst.*, vol. 35, no. 5, pp. 3529–3540, Sep. 2020.

[4] S. J. Geetha, S. Chakrabarti, and K. Rajawat, "Asynchronous hierarchical forecasting-aided state estimator with sub-area data validation for power systems," *IEEE Sensors J.*, vol. 21, no. 2, pp. 2124–2133, Jan. 2021.

[5] A. Abur and A. Gomez-Exposito, *Power System State Estimation: Theory and Implementation*. Boca Raton, FL, USA: CRC Press, 2004.

[6] Y.-F. Huang, S. Werner, J. Huang, N. Kashyap, and V. Gupta, "State estimation in electric power grids: Meeting new challenges presented by the requirements of the future grid," *IEEE Signal Process. Mag.*, vol. 29, no. 5, pp. 33–43, Sep. 2012.

[7] G. B. Giannakis, V. Kekatos, N. Gatsis, S.-J. Kim, H. Zhu, and B. F. Wollenberg, "Monitoring and optimization for power grids: A signal processing perspective," *IEEE Signal Process. Mag.*, vol. 30, no. 5, pp. 107–128, Sep. 2013.

[8] W. Zheng, W. Wu, A. Gomez-Exposito, B. Zhang, and Y. Guo, "Distributed robust bilinear state estimation for power systems with nonlinear measurements," *IEEE Trans. Power Syst.*, vol. 32, no. 1, pp. 499–509, Jan. 2017.

[9] X. Zhou, Z. Liu, Y. Guo, C. Zhao, J. Huang, and L. Chen, "Gradient-based multi-area distribution system state estimation," *IEEE Trans. Smart Grid*, vol. 11, no. 6, pp. 5325–5338, Nov. 2020.

[10] C. Wang, Z. Qin, Y. Hou, and J. Yan, "Multi-area dynamic state estimation with PMU measurements by an equality constrained extended Kalman filter," *IEEE Trans. Smart Grid*, vol. 9, no. 2, pp. 900–910, Mar. 2018.

[11] N. Xia, H. B. Gooi, S. Chen, and W. Hu, "Decentralized state estimation for hybrid AC/DC microgrids," *IEEE Syst. J.*, vol. 12, no. 1, pp. 434–443, Mar. 2018.

[12] C. Gómez-Quiles, H. A. Gil, A. de la Villa Jaén, and A. Gómez-Expósito, "Equality-constrained bilinear state estimation," *IEEE Trans. Power Syst.*, vol. 28, no. 2, pp. 902–910, May 2013.

[13] V. Kekatos and G. B. Giannakis, "Distributed robust power system state estimation," *IEEE Trans. Power Syst.*, vol. 28, no. 2, pp. 1617–1626, May 2013.

[14] A. Minot, Y. M. Lu, and N. Li, "A distributed Gauss-Newton methodfor power system state estimation," *IEEE Trans. Power Syst.*, vol. 31, no. 5, pp. 3804–3815, Sep. 2016.

[15] A. Gomez-Exposito, C. Gomez-Quiles, and A. de la Villa Jaen, "Bilinear power system state estimation," *IEEE Trans. Power Syst.*, vol. 27, no. 1, pp. 493–501, Feb. 2012.

[16] T. V. Cutsem, J. L. Horward, and M. Ribbens-Pavella, "A two level static state estimator for electric power systems," *IEEE Trans. Power App. Syst.*, vol. PAS-100, no. 8, pp. 34–35, 1981.
[17] Y. Wallach, E. Handschin, and C. Bongers, "An efficient parallel processing method for power system state estimation," *IEEE Power Eng. Rev.*, vol. PER-1, no. 11, pp. 20–21, Nov. 1981.
[18] G. N. Korres, "A distributed multiarea state estimation," *IEEE Trans. Power Syst.*, vol. 26, no. 1, pp. 73–84, Feb. 2011.
[19] J. Kang and D. Choi, "Distributed multi-area WLS state estimation integrating measurements weight update," *IET Gener., Transmiss. Distribution*, vol. 11, no. 10, pp. 2552–2561, Jul. 2017.
[20] Y. Guo, L. Tong, W. Wu, H. Sun, and B. Zhang, "Hierarchical multi-area state estimation via sensitivity function exchanges," *IEEE Trans. Power Syst.*, vol. 32, no. 1, pp. 442–453, Jan. 2017.
[21] L. Shan, J. Yu, J. Zhang, Y. Li, E. Zhou, and L. Zhao, "Distributed state estimation based on the realtime dispatch and control cloud platform," in *Proc. 2nd IEEE Conf. Energy Internet Energy Syst. Integr. (EI2)*, Oct. 2018, pp. 1–6.
[22] Y. Chen, J. Ma, P. Zhang, F. Liu, and S. Mei, "Robust state estimator based on maximum exponential absolute value," in *Proc. IEEE Power Energy Soc. Gen. Meeting*, Chicago, IL, USA, Jul. 2017, p. 1.
[23] W. Wu, Y. Guo, B. Zhang, A. Bose, and S. Hongbin, "Robust state estimation method based on maximum exponential square," *IET Gener., Transmiss. Distribution*, vol. 5, no. 11, pp. 1165–1172, 2011.
[24] T. Chen, H. Ren, E. Y. S. Foo, L. Sun, and G. A. J. Amaratunga, "A fast and robust state estimator based on exponential function for power systems," *IEEE Sensors J.*, vol. 22, no. 6, pp. 5755–5767, Mar. 2022.
[25] G. Yang, P. Dong, M. Liu, and H. Wu, "Research on random fuzzy power flow calculation of AC/DC hybrid distribution network based on unified iterative method," *IET Renew. Power Gener.*, vol. 15, no. 4, pp. 731–745, Mar. 2021.
[26] A. M. O. Mohamed and R. El-Shatshat, "Sequential network-flow based power-flow method for hybrid power systems," *IET Gener., Transmiss. Distribution*, vol. 15, no. 16, pp. 2384–2395, Aug. 2021.
[27] V. Donde, X. Feng, I. Segerqvist, and M. Callavik, "Distributed state estimation of hybrid AC/HVDC grids by network decomposition," *IEEE Trans. Smart Grid*, vol. 7, no. 2, pp. 974–981, Mar. 2016.
[28] X. Kong, Z. Yan, R. Guo, X. Xu, and C. Fang, "Three-stage distributed state estimation for AC-DC hybrid distribution network under mixed measurement environment," *IEEE Access*, vol. 6, pp. 39027–39036, 2018.
[29] R. Jegatheesan and K. Duraiswamy, "AC/multi-terminal DC power system state estimation—A sequential approach," *Electric Mach. Power Syst.*, vol. 12, no. 1, pp. 27–42, 1987.
[30] L. Roy, A. K. Sinha, and H. N. P. Srivastava, "Static state estimation of multiterminal DC/AC power system in rectangular coordinates," *Electric Mach. Power Syst.*, vol. 19, no. 1, pp. 69–80, 1991.

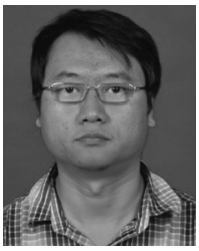

HAIBO ZHANG (Senior Member, IEEE) was born in Heilongjiang, China, in 1975. He received the Ph.D. degree from the Department of Electrical Engineering, Tsinghua University, Beijing, in 2005. His current research interests include energy management systems (EMSs) and new energy power system planning, operation, and control.

HOUYU QI was born in Henan, China, in 2001. He is currently pursuing the master's degree with North China Electric Power University, Beijing, China. His current research interest includes power system optimization operation.

SHUAI WANG (Member, IEEE) was born in Hunan, China, in 1996. He received the master's degree from North China Electric Power University, Beijing, China, in 2021. His current research interest includes distributed power flow.